https://doi.org/10.2352/ISSN.2169-4451.2018.34.107

Inkjet Printing platforms for DNA-based pathogen detection

Min Zhao, School of Electrical and Computer Engineering, Purdue University, West Lafayette, IN, USA
Susana Diaz Amaya, Seon-ah Jin, Li-Kai Lin, School of Materials Engineering, Purdue University, West Lafayette, IN, USA
Amanda J. Deering, Department of Food Science, Purdue University, West Lafayette, IN, USA
Lia Stanciu, School of Materials Engineering, Purdue University, West Lafayette, IN, USA
George T.-C. Chiu, School of Mechanical Engineering, Purdue University, West Lafayette, IN, USA
Jan P. Allebach, School of Electrical and Computer Engineering, Purdue University, West Lafayette, IN, USA

Abstract

Printing technologies recently have been applied to environmental pollution and food safety testing applications because there is more and more demand for inexpensive, portable and functional devices to be used for monitoring food and environment, such as enzyme-based biosensors [1] [2]. A system for printing nanoliter DNA based solution droplets on a lateral flow test strip with improved sensitivity for detection of Escherichia coli O157:H7 (E.coli O157:H7) is described in this article. We will present an overview of the results obtained with our printing process and the image analysis of the responses in the test strips. The printing process includes the precise control of droplet volume, the design of the print masks, and functional printing of the DNA-based solution. We create an image analysis system to read the responses of the test strips to the foodborne pathogens (Escherichia coli O157:H7) and determine the relationship between the responses and the concentration of the E.coli. Furthermore, we confirm that our printed test strips can successfully detect the presence of E.coli O157:H7 with a concentration as low as 10^2 *CFU/ml.*

Introduction

Inkjet printing has been around for several decades. The most popular application of this printing technology has been to print paper documents containing text and graphics. From the mid-1990s, the field of bio-printing began to grow, with a rapid increase after 2000 because inkjet printers began to be used for dispensing functional materials. The incorporation of printing technology with biomaterials has recently gained considerable attention. For instance, printing technique has been used for the regeneration of bone or ear tissues [3] [4]. Inkjet printing is an advanced technique enabling the deposition of various kinds of solutions (biomolecules, polymers, metals) onto different types of substrates (cellulose, polymer, silicon.). It enables fast printing of any computer-generated pattern onto substrates by precise placement of pico-to-nanoliter volumes of inks [5].

Recently printing technologies have become very popular in environmental pollution and food safety testing applications. According to the World Health Organization (WHO), there are estimated 600 million people falling ill after eating contaminated food and 420 thousands death every year [6]. The most common foodborne pathogens include Salmonella, Campylobacter, and Enterohaemorrhagic Escherichia coli. Among these foodborne pathogens, *E.coli* O157:H7 can be easily found in contaminated water and contaminated food, especially undercooked ground beef, milk and juice, raw fruits and vegetables. It is known that *E.coli* O157:H7 can cause bloody diarrhea and sometimes cause kidney failure and even death. Therefore, an affordable, rapid and simple method for detecting *E.coli* O157:H7 is more and more in demand. The manufacturing process of inkjet printing can guarantee rapid, reliable, and reproducible mass production of functional biosensors with specific detection properties at low cost.

The goal of our research is to design printed test strips (PTSs) to be used for the detection of *E.coli* O157:H7. Each functional PTS with two printed lines: the test line and the control lines, is intended to be affordable, portable, sensitive, rapid, and easy-to-use. Natural cellulose paper (Hi-flow HFC075, EMD Milipore, www.emdmilipore.com) is the substrate and the printing consists of two types of DNA-based biomaterial (the biomaterial on test lines, control lines: Carboxyl functionalized Aptamer sequence, and Biotin DNA complementary sequence, respectively). To precisely control the amount of the DNA solution and to design a system for reproducible mass production, a piezoelectric inkjet printer PipeJet (BioFluidiX, Freiburg, Germany) with deposition of single droplets in the range of 2 - 70 nL is used to print DNA solution onto the substrates. The focus of the functional printing part is to develop processes for inkjet and roll-to-roll patterning of nano-functionalized biocompatible and biodegradable cellulose test strips, therefore enabling the efficient manufacture of food pathogen biosensors. To date, we have fabricated and used the PTSs to successfully detect the presence of foodborne pathogens (*E.coli* O157:H7), and confirm an immune detection limit of 10^2 CFU/ml.

In this work, we develop the inkjet printing process for producing the pattern for the capture of *E.coli* O157:H7, and design an image analysis method to detect the responses in test lines of test strips. In the following sections, we first characterize the consistent size droplets to design the print mask, functional print the test and control lines with the corresponding solutions. We then detect *E.coli* O157:H7 with different concentrations to validate our approach by showing the responses in test lines and control lines of the PTSs. Our image analysis method has a quantitative metric to characterize the responses in test lines of the images captured by a mobile camera.

Experimental Details

Printing parameters that influence the fabrication process include the print mode, print mask, and number of print passes. To have a better print quality, consistent droplets without satellites are required [7]. To design the print masks for the DNA-based solution, the average droplet volume and the average diameter of the deposited droplets on the substrate need to be known.

System

The inkjet system used for our current work is shown in Figure 1. This system consists of an XY motorized stage (Anorad WKY-150) with an encoder resolution of 0.5 μm, a stationary PipeJet piezoelectric droplet ejection system with one nozzle diameter of 200 μm that can eject a single droplet in the range of

2 - 70 nL at an ejection frequency ranging from 1 to 100 Hz, and an optical system for ink ejection visualization [8]. We use a visual C-based printing software package to read an input bitmap image and pixel resolution, then correlate the controller with dot positions. The controller sends trigger signals of ejection to the printer at prescribed addresses when the stage moves beneath the printer [9][10].

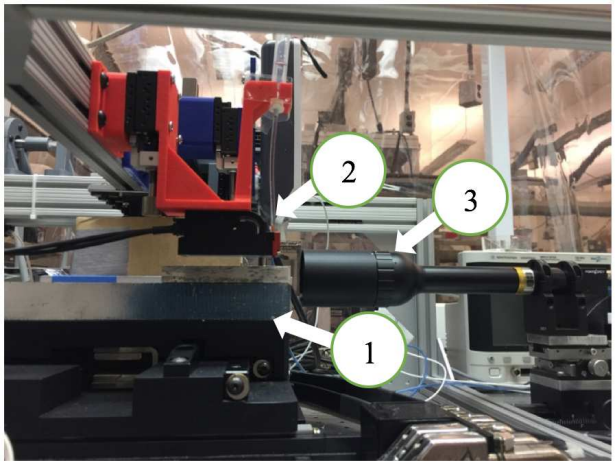

Figure 1. *Inkjet system includes: (1) An XY motorized stage, (2) A PipeJet printer, (3) An optical system.*

Consistent Droplets and its volume

One of the sources of artifacts in the inkjet process is the creation of satellites, which occurs due to the separation of ink emerging from the nozzle exit. To view the ejection result, we set up an optical system, as illustrated in Figure 2 [9]. The optical system mainly consists of a PipeJet Inkjet System, a SPiiPlus Series motion controller, a stroboscope light, a CCD camera (Point Grey Flea3 USB3.0: FL3-GE-13Y3M-C), and a three-axis optical table (NRC pneumatic isolation table type XL-A). A PipeJet with one nozzle is installed on the top of the three-axis table and the nozzle exit is oriented toward gravity. The controller sends the trigger signals to the printer, and also sends the delay unit trigger signals to the stroboscope light. After the printer receives the trigger signal, the images of the ejected droplets can be captured by the CCD camera, displayed on the monitor screen, and stored in a file.

The printing system can be tuned to product droplets without satellites. As we tune the printing parameters (stroke and stroke velocity) during the ejection process, the printing results can be recorded, as illustrated in Figures. 3(a) and 3(b). The stroke is the ratio of the piston displacement to the maximus displacement, and the stroke velocity is the velocity of the displacement of the piston.

In our experiment, the frequency of the firing is fixed at 100 Hz, the dispensing nozzle is Pipe 200, and the operating Stroke and Stroke velocity are varied in a range from 0 to 100% with an increment of 10%, and 0 to 100 μm/ms with an increment of 10, respectively.

We record and apply those qualified printing parameters to compute the average droplet mass by depositing 500 drops of ink into a clean vial, the mass of which is measured before deposition and after deposition. We ignored the evaporation loss since the time interval before and after deposition was took 5 seconds. The droplet volume equals the mass divided by its density.

Dot Analysis

To measure the average diameter of the drops after impacting the substrate, we first design a test pattern which can quantify the measurement of the dot size, and the presence or absence of satellites.

The test pattern we designed is a 10×10 pixel grid of single drops, each separated by a single pixel. Hence, there are a total of 100 dots in the test pattern, as illustrated in Figure 4(a) [11]. The print mode parameters used to print the test pattern are as follows:

Printing frequency: 100 Hz, Stroke: 100%, Stroke velocity: 100 μm/ms, Unidirectional printing, Media advance speed: 2 mm/s, Media return speed: 20 mm/s, Nozzle resolution: 200 μm, Ink: black ink (BCH), Substrate: Hi-flow HFC075, Standoff distance between the print head and the substrate: 1 mm.

Then we scan the printed test pattern using an EPSON 10000XL (Epson America, Inc., Long Beach, CA, USA) flatbed scanner with resolution 1000 dpi, and obtain the grayscale image, as illustrated in Figure 4(b). The threshold for the image binarization is calculated using Otsu's method to find the threshold that maximizes the between-class variance [12]. Figure 4(c) shows the corresponding binary image. We then find the boundaries delimiting dot regions by vertically and horizontally projecting the data of the binary image, as illustrated in Figure 4(d). With the aid of these boundaries, we can calculate the total number of nonzero pixels for each dot. The average diameter of the dots can be calculated using the following equation, assuming that each dot is circular.

$$\mathrm{D} = \sqrt{\frac{4 \cdot N \cdot S}{\pi}}, \tag{1}$$

where N is the number of pixels of a dot, and S is the area of a pixel.

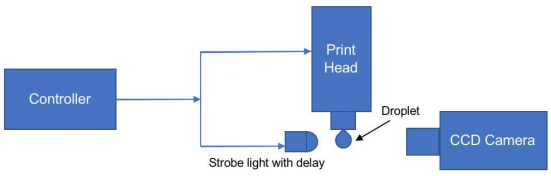

Figure 2. *A schematic view of the optical system for viewing droplet formation.*

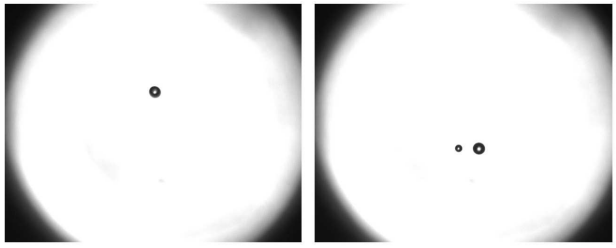

Figure 3. *(a) The process of DI water drop ejection when the stroke and the stroke velocity equal 0% and 80 μm/ms, respectively, resulting in only one droplet. (b) The process of DI water drop ejection when the stroke and the stroke velocity equal 0% and 90 μm/ms, respectively, resulting in one main droplet and a satellite.*

Print Mask Design

According to the requirements of the printed volume and the size of each test or control line, we can design the print mask and the number of printing cycles. The print head of a PipeJet printer consists of one nozzle which enables printing patterns to be easily formed.

The number of the droplets in the horizontal (vertical) direction equals the length (width) of the test line divided by the average diameter of the dots, and the number of the printing cycles equals the total target printed volume of a test line divided by the total volume of a printing cycle. The calculation process is similar for a control line, except that the bio-inks are different.

Figure 5 shows the print mask, which consists of two print patterns to be applied to the test line. The optimized print mask provides better control of the printed DNA pattern. The numbers in the print mask represent the sequence of the print-head passes over the substrate. We spread out the drops to increase the time between the printing of adjacent pixels. Here is how we define a cycle (or a layer): print one pass of pattern A, then print one pass of pattern B. In our work, the number of cycles for the test line printing is 15.

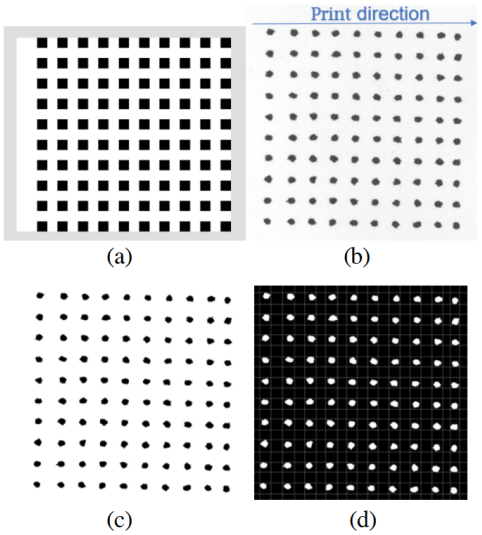

Figure 4. *(a) Test pattern for dots characterization, (b) Print result of test pattern scanned at 1000 dpi with EPSON 10000XL with no satellites, (c) Corresponding binary image, (d) Boundaries delimiting dot regions shown in white.*

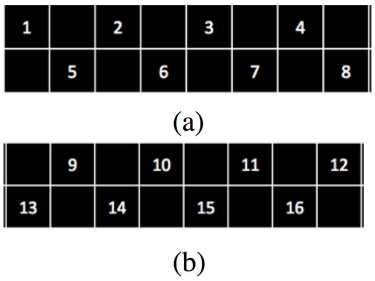

Figure 5. *Print mask used to control the printing of a 4 mm x 1 mm line of DNA solution. The printing is done in two passes defined as a cycle, using pattern (a) and pattern (b), in sequence. Therefore, for a cycle, eight droplets are ejected in each row and two droplets are ejected in each column.*

Bio-printing Experiment and Test Results

For each test line and control line, pathogen capture arrays are printed using the printing system with corresponding colorless bio-inks and the designed print patterns described above. To verify that the PTS is functioning, we apply Aptamer-based assay test technology to the PTSs to detect *E.coli* O157:H7 with different concentrations.

We describe the Aptamer-based assay test as follows: we add the Au-Ps particles (Gold decorated Polysterene) in a solution with *E.coli* O157:H7, then drop the mixed solution on the absorption pads (the end near to the test lines) of the PTSs [6]. The mixed solution will be drawn from the test zone to the control zone through capillary phenomena. After 20 minutes, two pink zones appear on each PTS. The test interpretation is described as follows: the pink test line in the test zone is used to confirm the presence of *E.coli* O157:H7, and the control lines are designed to confirm the functioning of the PTSs because the pink control line still appears when the mixed solution without *E.coli* O157:H7 reaches the control zone .

Figures 6(a) and 6(b) show the test results of the PTSs used to detect the concentration of *E.coli* O157:H7 with 0, $10^3, 10^4, 10^5$, and 10^6 CFU/ml, respectively. The visible responses in the control lines and test lines indicate that the PTS is able to sucessfully capture the *E.coli* O157:H7. To determine the detection limit, another ten PTSs are used to detect the concentration of *E.coli* O157:H7 with 10^2 CFU/ml. After doing the Aptamer-based assay test on these PTSs, the pink lines appeared on the test lines and the control lines, as illustrated in Figures 7(a) and 7(b). Therefore, we prove that our PTSs can capture *E.coli* O157:H7 with limits of detection down to 10^2 CFU/ml.

Image Analysis via A Cell Phone Camera

We propose an image analysis method to assess the responses by using a mobile phone camera. The metric that we used to characterize the responses in test lines of the test strips in this approach is the grayscale values, which is the sum of the CIE ΔE values of the test line. The image of the test strips was captured in a Macbeth SpectraLight II light booth (Gregtag Macbeth, New Windsor, NY, USA)) for providing the daylight environment with a mobile phone camera, as illustrated in Figure 6(a). The test zone images and the corresponding background images were cropped and scaled to 60×130, and 60×40 pixels, respectively, using Adobe Photoshop and saved in TIFF format without compression, as illustrated in Figure 6(b). We transform the gamma-corrected sRGB values of these five images to linear RGB values according to Eq. (2) [13].

$$I_{linear} = \begin{cases} \frac{I_{sRGB}/255}{12.92}, & (I_{sRGB}) \leq 0.03928 \\ \left(\frac{I_{sRGB}/255+0.055}{1+0.055}\right)^{2.4}, & otherwise \end{cases} \quad (2)$$

Then, these linear RGB values are converted into CIE XYZ values in the matrix transformation step.

$$\begin{bmatrix} X \\ Y \\ Z \end{bmatrix} = \begin{bmatrix} 0.4124 & 0.3576 & 0.1805 \\ 0.2126 & 0.7151 & 0.0721 \\ 0.0193 & 0.1192 & 0.9505 \end{bmatrix} \begin{bmatrix} R_l \\ G_l \\ B_l \end{bmatrix}. \quad (3)$$

We then transform CIE XYZ to the CIE L* a* b* color space which is a uniform color space.

$$\begin{aligned} L^* &= 116 \times f(\tfrac{Y}{Y_n}) - 16 \\ a^* &= 500 \times [f(\tfrac{X}{X_n}) - f(\tfrac{Y}{Y_n})] \\ b^* &= 200 \times [f(\tfrac{Y}{Y_n}) - f(\tfrac{Z}{Z_n})]. \end{aligned} \quad (4)$$

Here, $[X_n, Y_n, Z_n]$ is the reference white point, and $f(t)$ is given by

$$f(t) = \begin{cases} t^{\frac{1}{3}}, & t > \left(\frac{6}{29}\right)^3 \\ \frac{1}{3} \cdot \left(\frac{19}{6}\right)^2 t + \frac{4}{29}, & otherwise \end{cases} \quad (5)$$

To obtain the corresponding gray scale images, we compute the ΔE value from the background which is the color difference between the pixel values and the local background.

$$\Delta E = \sqrt{(L^* - L_{avg})^2 + (a^* - a_{avg})^2 + (b^* - b_{avg})^2}, \quad (6)$$

where $(L_{avg}, a_{avg}, b_{avg})$ are the average values from the local background. Then we normalize the ΔE values of the images to the range [0,255] [14][15].

Figure 6(c) shows the original RGB images and the corresponding grayscale images. We use Otsu's method to get the initial binary images. To get the final version of the binary images, we use the 4-point connected component method to remove noise by calculating the area of each component and making sure that the pixel values of the largest area are 1, while the rest is 0. Figure 6(d) shows the original RGB images and the final version of the binary images. With the aid of the binary images, the location of the responses in the test lines can be defined. We use grayscale values as a metric, calculating the sum of ΔE values of the test lines, to characterize the responses in the test lines. Figure 6(e) shows the relationship between the grayscale values and the concentration of *E.coli* O157:H7.

To assess the variation among the responses in test lines of test strips by correlating the color intensity under a fixed concentration of 10^2 CFU/ml, we do the same image analysis on the 10 test strips to obtain the grayscale images and the corresponding binary images, as illustrated in Figures 7(c) and 7(d). The color intensity on the test lines on different strips appears differently because of the variance of the mesh structure, the flow path, and the shape of the test strips. Figure 7(e) shows a plot of the variation among the responses of the test lines at the same concentration.

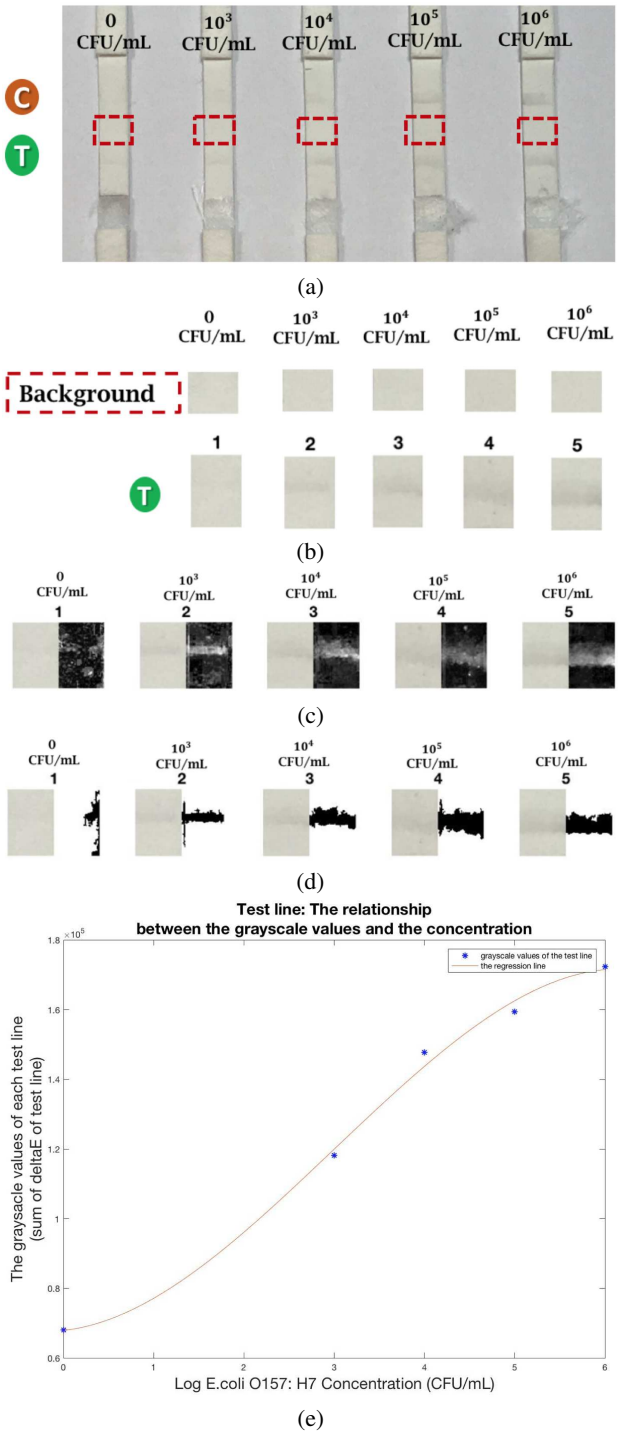

Figure 6. *(a) The test results of the PTSs used to detect the different concentrations of E. coli O157:H7. The image is captured by a mobile phone (iPhone 7 Plus). (b) Cropped version of test zones and the local background of the test strips. (c) The original RGB images of the test zones and the corresponding grayscale images. (d) The original RGB images of the test zones and the final version of the corresponding binary images. (e) The plot of the relationship between the grayscale values and the concentration of E. coli O157:H7.*

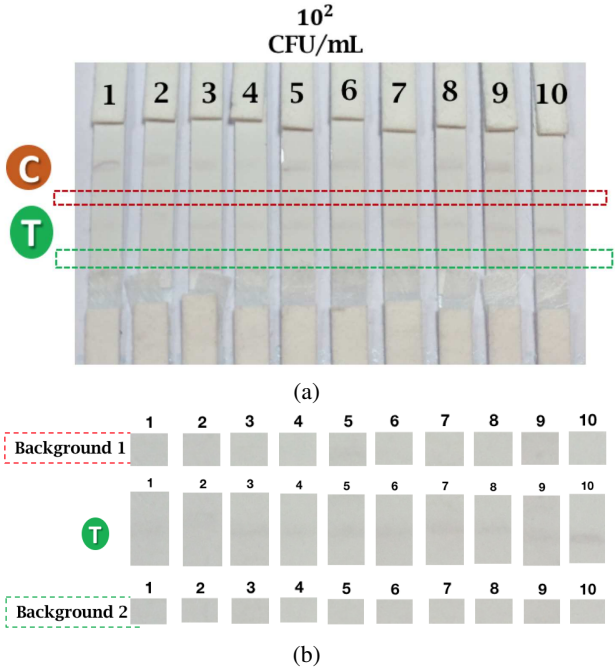

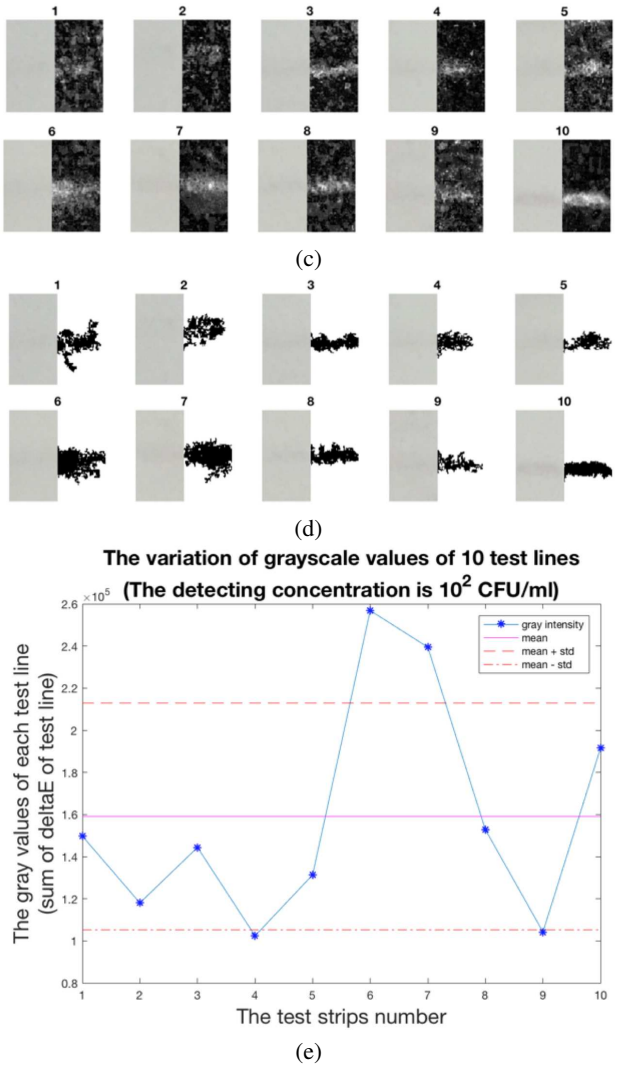

Figure 7. *(a)Test results of PTSs used to detect E. coli O157:H7 with the concentration* 10^2 *CFU/ml. The image is captured by a mobile phone (iPhone 6 Plus). (b) Cropped version of test zones and two types of local background of the test strips. (c) The original RGB images of the test zones and the corresponding grayscale images. (d) The original RGB images of the test zones and the final version of the corresponding binary images. (e) The plot of the variation of the grayscale values as a function of test strip number. The mean and standard deviation of the sum of* ΔE *value across the 10 test strips are* $1.59x10^5$ *and* $1.59x10^5$*, respectively.*

Conclusion

In this paper, we propose a system for printing test strips to detect foodborne pathogens, and imaging processing algorithms to analyze images of the exposed test strip that have been captured with a mobile phone camera. The image processing algorithms are designed to detect the presence a pathogen, and to estimate its concentration. The overall goal of the project is to develop a test system that is low-cost, and simple enought to implement in the field. We believe that printing offers a manufacturing method that is low-cost, reliable, and scalable. To date we have worked only with *E.coli* O157:H7. But we believe that our framework could be applied to other food-borne pathogens, as well.

We show that the functioning PTS can detect the presence of foodborne pathogens and confirm an Aptamer-based assay detection limit of 10^2 CFU/ml. The relationship between the optical properties of the test lines and the different concentrations of the pathogen is also investigated. Further research can include the optimization of printing layers that can reduce material (bio-inks) cost and printing time, as well as an effort to reduce the sample-to-sample variation in the response to low concentrations of *E.coli* O157:H7.

Acknowledgments

This manuscript is based upon work supported by the U.S. Department of Agriculture, Agricultural Research Service, under Agreement No. 59-8072-6-001. Any opinions, findings, conclusion, or recommendations expressed in this publication are those of the author(s) and do not necessarily reflect the view of the U.S. Department of Agriculture.

We thank Runzhe Zhang and Jie Wang for their assistance with the printing experiments and the set-up of the printing system.

References

[1] M. Tudorache and C. Bala, Biosensors based on screen-printing technology, and their applications in environmental and food analysis, Analytical and Bioanalytical Chemistry, p. 565. (2007).

[2] A. Othman, A. Karimi, and S. Andreescu, Functional nanostructures for enzyme based biosensors: properties, fabrication and applications, Journal of Materials Chemistry B, p. 7178. (2016).

[3] JS. C. Ligon, R. Liska, J. Stampfl, M. Gurr, and R. Mulhaupt, Polymers for 3D printing and customized additive manufacturing, Chemical Reviews, p. 10212. (2017).

[4] J. Credou, R. Faddoul, and T. Berthelot, Photo-assisted inkjet printing of antibodies onto cellulose for the eco2-friendly preparation of immunoassay membranes, RSC Advances, p. 29786. (2015).

[5] J. T. Delaney, P. J. Smith, and U. S. Schubert, Inkjet printing of proteins, Soft Matter, p. 4866. (2009).

[6] S. A. Jin, Y. Heo,L. K. Lin, A. J. Deering, G. T. Chiu, J. P. Allebach, and L. A. Stanciu, Gold decorated polystyrene particles for lateral flow immunodetection of Escherichia coli O157:H7, Microchimica Acta, p. 4879. (2017).

[7] J. P. Allebach, G. Y. Lin, C. L. Chen, G. T. C. Chiu, F. A. Baqai, J. H. Lee, Image analysis as a tool for printer characterization and halftoning algorithm development, IEEE, p. 0003. (2002).

[8] T. Bhuvana, W. Boley, B. Radha, B.D. Dolash, G. Chiu, D. Bergstrom, R. Reifenberger, T.S. Fisher, G.U. Kulkarnil, Inkjet printing of palladium alkanethiolates for facile fabrication of metal interconnects and surface-enhanced Raman scattering substrates, Micro & Nano Letters, p. 296. (2010).

[9] P.-H. Chen, W.-C. Chen, and S.-H. Chang, Bubble growth and ink ejection process of a thermal ink jet printhead, International Journal of Mechanical Sciences, p. 683. (1997).

[10] A. K. Adak, J. W. Boley, D. P. Lyvers, G. T. Chiu, P. S. Low, R. Reifenberger, and A. Wei, Label-free detection of Staphylococcus aureus captured on immutable ligand arrays, ACS Applied Materials & Interfaces, p. 6404. (2013).

[11] E. Bernal, J. P. Allebach and Z. Pizlo, Improved pen alignment for bidirectional printing, Journal of Imaging Science and Technology, p. 001. (2007).

[12] N. Otsu, A threshold selection method from gray-level histograms, IEEE Transactions on Systems, Man, and Cybernetics, p. 62. (1979).

[13] Y. Ju, E. Maggard, R. Jessome, and J. Allebach, Autonomous detection of text fade point with color laser printers, Proc. SPIE. vol. 9396. (2015).

[14] Y. Lei, Camera/projector-based document/object capture system

using structured light: reflectance map image quality assessment and design of structured light patterns and analysis algorithms, Ph.D. Thesis, Purdue University. (2014).
[15] W. Wang, A study on image quality evaluation in image capture and production process, Ph.D. Thesis, Purdue University. (2016).

Author Biography

Min Zhao is a graduate student in Electrical and Computer Engineering at Purdue University under the supervision of Professor Jan P. Allebach. She received her B.S. degree in Mechanical Engineering from Qingdao Technology University, Shandong, China. Now, her current research interests include bio-printing and image analysis.